International Journal of Solids and Structures xxx (xxxx) xxx

Contents lists available at ScienceDirect

International Journal of Solids and Structures

journal homepage: www.elsevier.com/locate/ijsolstr

Grain size-dependent energy partition in phase transition of NiTi shape memory alloys studied by molecular dynamics simulation

Kai Nie[a], Ming-Peng Li[a], Wen-Ping Wu[a,*], Qing-Ping Sun[b,*]

[a] Department of Engineering Mechanics, School of Civil Engineering, Wuhan University, Wuhan 430072, China
[b] Department of Mechanical and Aerospace Engineering, The Hong Kong University of Science and Technology, Hong Kong, China

ARTICLE INFO

Article history:
Received 11 November 2019
Revised 6 February 2020
Accepted 17 February 2020
Available online xxx

Keywords:
Energy partition
Phase transition at nano-scale
Shape memory alloys
Grain size effects
Molecular dynamics simulation

ABSTRACT

Nanocrystalline NiTi shape memory alloys show fundamental changes in phase transition behavior when the grain size is reduced down to nano-scale (grain size<30 nm). However, due to the extreme difficulties of in-situ experimental observation, universally acknowledged physical mechanisms and detailed microstructures at atomic level are still not clear. In this paper, detailed microstructure images and quantified energy partition at atomic level during stress-induced phase transition are obtained by molecular dynamics simulation. Phase transition is gradually suppressed and incomplete phase transition occurs as grain size decreases. The potential energy landscape of the nanocrystalline system changes significantly from nonconvex to convex, which leads to corresponding changes in stress–strain response and microstructural evolution. With decreasing grain size, the interface (grain boundary and phase boundary) energy makes much more contributions in variation of the system potential energy than the crystallite (austenite and martensite) energy. The mechanism of energy dissipation changes from atomic interface friction in phase transition to plastic deformation caused by grain boundary sliding. It is the gradual dominance of interfacial energy terms in total potential energy that leads to the observed fundamental changes of phase transition behavior in nanocrystalline NiTi.

© 2020 Elsevier Ltd. All rights reserved.

1. Introduction

As a typical shape memory alloys (SMAs), polycrystalline NiTi alloy is applied in many fields due to shape memory effect and superelasticity (pseudoelasticity) of the material (Duerig et al., 1999; Morgan, 2004; Saadat et al., 2002; Humbeeck, 1999). When grain size of NiTi is reduced down to nano-scale (especially less than 30 nm), increased volume fraction of grain boundary phase significantly affect the phase transition and mechanical behaviors of nanocrystalline (NC) NiTi SMAs (Sun et al., 2014; Mousavi et al., 2008; Yin et al., 2016; Ahadi et al., 2017). The phase transition under stressing or cooling is significantly suppressed as the grain size is decreased below a critical value. The reduction of grain size down to nanoscale has led to novel properties (such as extremely small hysteresis, high strength) of NC NiTi SMAs as reported in the literature (Ahadi and Sun, 2013; Ahadi and Sun, 2014; Ahadi and Sun, 2015; Ahadi and Sun, 2016; Waitz et al., 2004). However, the exact underlying physical mechanism and the detailed microstructure evolution at nano-scale are not yet fully understood and clearly demonstrated.

The dominance of interfacial effects has been proposed to play important role in the phase transition behavior of NC NiTi. For polycrystalline SMAs, it is more difficult to induce phase transition of the crystallite by stress near grain boundary or triple junction because of their strong constraint to the crystallites (Ueland and Schuh, 2013). The phase transition is gradually suppressed and the stress–strain hysteresis loop area decreases gradually as the grain size decreases (Sun et al., 2014). Meanwhile, the morphology of martensite also changes in NC SMAs (Waitz et al., 2009). There is no coexistence of two phases (austenite and martensite) during phase transition inside a nanosized grain (Ahadi and Sun, 2015). The phase transformation band and the sharp interface between austenite and martensite are not found in nanosized grains but are observed clearly during phase transition process in the coarse grain NiTi (Miyazaki et al., 1981; Mao et al., 2010; Reedlunn et al., 2014; Shaw and Kyriakides, 1997). In-situ diffraction results indicated that phase transition at extremely small scale is realized through a continuous lattice distortion (Ahadi and Sun, 2015) and

* Corresponding authors.
E-mail addresses: wpwu@whu.edu.cn (W.-P. Wu), meqpsun@ust.hk (Q.-P. Sun).

https://doi.org/10.1016/j.ijsolstr.2020.02.027
0020-7683/© 2020 Elsevier Ltd. All rights reserved.

Please cite this article as: K. Nie, M.-P. Li and W.-P. Wu et al., Grain size-dependent energy partition in phase transition of NiTi shape memory alloys studied by molecular dynamics simulation, International Journal of Solids and Structures, https://doi.org/10.1016/j.ijsolstr.2020.02.027

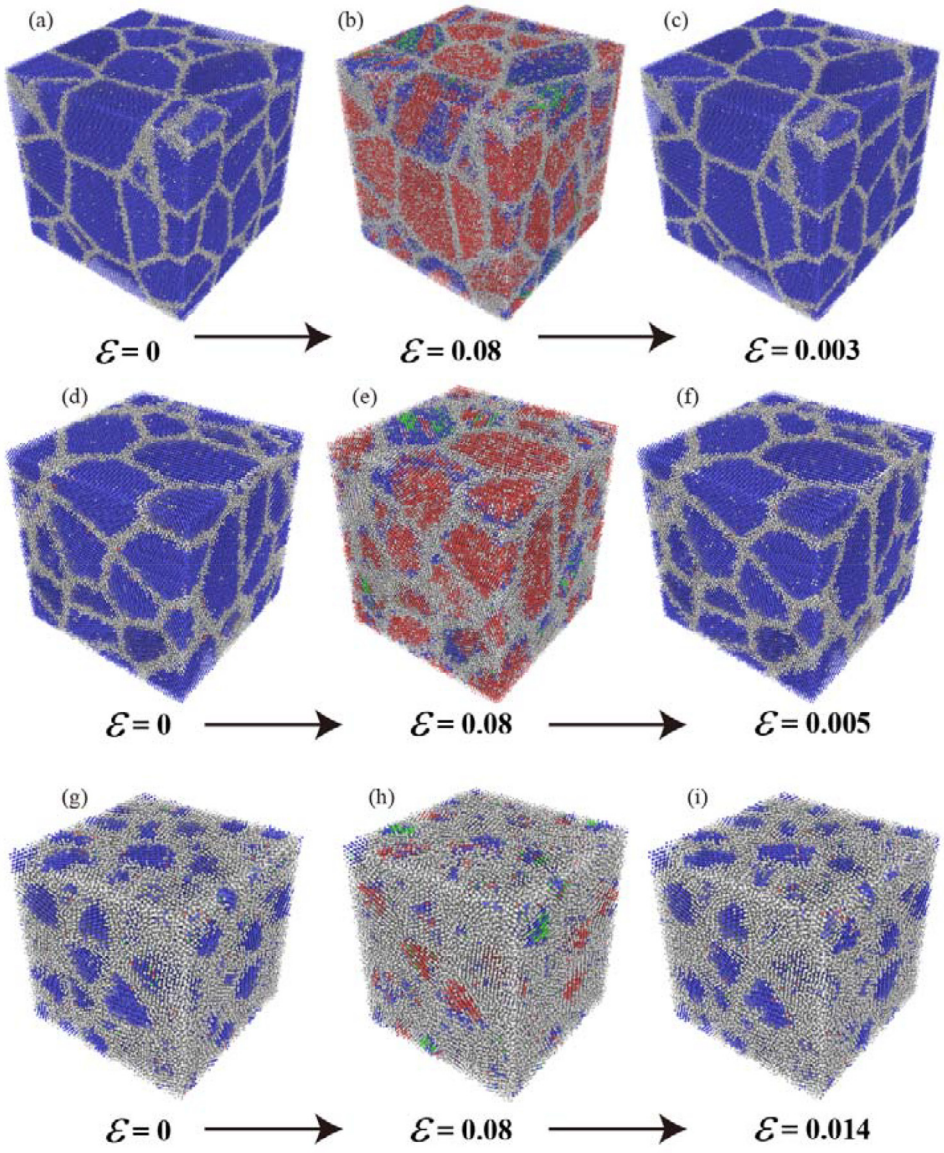

Fig. 1. Images of the microstructure change in loading and unloading in the samples with the grain size of 11.97 nm ((a)–(c)), 7.98 nm ((d)–(f)) and 4.02 nm ((g)–(i)).

the traditional nucleation-and-growth mode of phase transition and two phase coexistence may break down in NC NiTi (Dong and Sun, 2009; Dong et al., 2016; Truskinovsky and Zanzotto, 1996).

To describe the fundamental changes of phase transition behavior in NC NiTi due to grain size reduction, nonlocal 1D effective continuum model is introduced to study the grain size effects by considering the roles of grain size, grain boundary thickness and phase boundary thickness in previous work (Li and Sun, 2018). Useful insights are provided to understand the nanoscale phase transition phenomena. It is shown that the phase transition under stress is indeed gradually suppressed when the grain size is reduced to nano-scale. The free energy landscape changed from non-convex to convex when the grain size is reduced to a critical value. Grain boundary energy becomes the dominant energy term and leads to the breakdown of two-phase (austenite and martensite) coexistence and the decrease of hysteresis loop area of NC NiTi. However, detailed nanoscale physical pictures of the phase transition process are still missing in the literature.

To overcome the difficulties in the observation of the microstructure evolution in experiment and in quantitative nano and atomic scale energy analysis by continuum methods, molecular dynamics (MD) simulation has been used to provide valuable information and support for exploring micro-mechanism, nanoscale morphology and energy evolution during phase transition process in NC NiTi (Chowdhury et al., 2015). Meanwhile, MD simulation can also serve as an effective bridge between the continuum model prediction and experiment phenomenon. The phase transition behavior of NiTi single crystal and NiTi nanopillar are studied by MD simulations (Chowdhury et al., 2015; Zhong et al., 2012; Wang et al., 2017; Yin et al., 2015; Ma et al., 2017; Chen et al., 2017; Muralles et al., 2017). The second nearest neighbor modified embedded atom method potential (2NN MEAM) developed by Ko et al. (Ko et al., 2015) is employed to investigate the temperature/stress induced phase transition behavior with improved accuracy. It is found that phase transition was gradually suppressed with grain size reduction by MD simulation (Ko et al., 2017). Nevertheless, the underlying mechanism of grain size dependent phase transition behavior in the MD simulations still remains largely speculative. In particular, how the grain boundary and the phase boundary quantitatively contribute to the system energy and affect the phase transition process are still not very clear.

Please cite this article as: K. Nie, M.-P. Li and W.-P. Wu et al., Grain size-dependent energy partition in phase transition of NiTi shape memory alloys studied by molecular dynamics simulation, International Journal of Solids and Structures, https://doi.org/10.1016/j.ijsolstr.2020.02.027

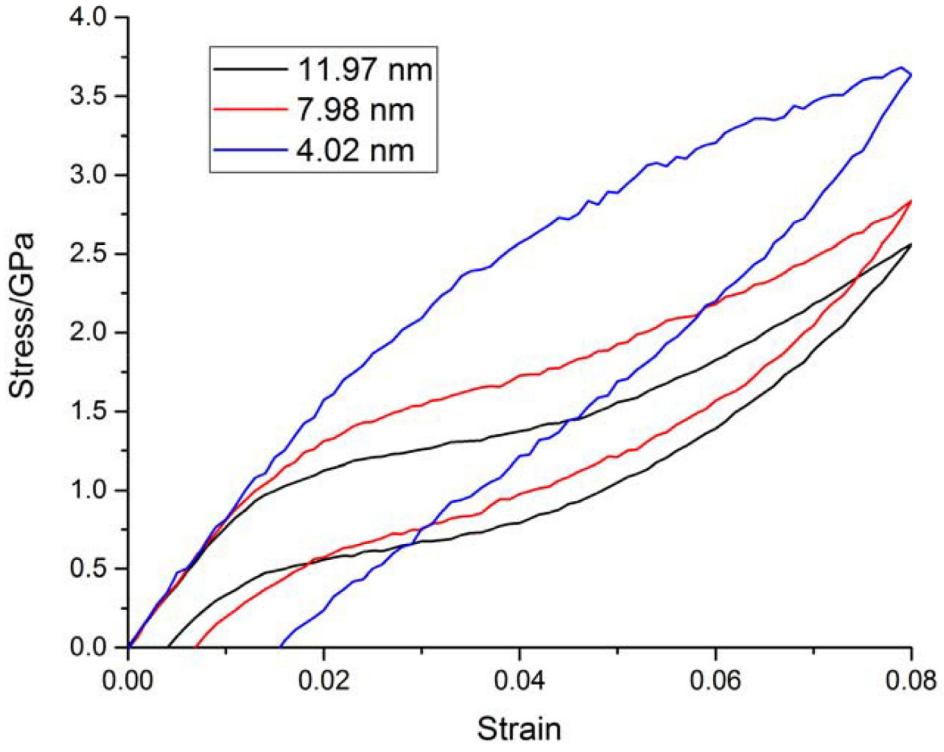

Fig. 2. Stress–strain curves in the samples of different grain sizes.

In this paper, detailed atomic pictures of the microstructure evolution and the system energy are obtained by MD simulations. Based on the calculated energies of austenite, martensite, grain boundary, and phase boundary and their percentage in total energy variation, the contribution of interface (grain boundary and phase boundary) to the system energy and therefore to the macroscopic response are quantified.

2. NC NiTi models and MD simulation

NC NiTi models with three different grain sizes (4.02 nm, 7.98 nm, and 11.97 nm) are built in this paper by Atomeye software (http://li.mit.edu/Archive/Graphics/A/utils.html) as shown in Table 1. The thickness of the grain boundary in all the models is about 1 nm which is about three times of the lattice constant of NiTi. To avoid the surface effect, the periodic boundary conditions are applied in all the three directions of each model. The 2NN MEAM potential (Ko et al., 2015) is used in the MD simulation with time step of $2 \times 10^{-15}s$. The models are first relaxed at 400 K in the NPT (the total number of particles (N), the total pressure (P) and the temperature (T) are constant) ensemble where the austenite is stable since 400 K is higher than the austenite finish temperature (A_f). Then displacement-controlled uniaxial tensile loading and unloading are applied to the NPT ensemble with a nominal overall strain rate of $5 \times 10^{8}s^{-1}$ and the maximum strain of 8%. The atomic configurations and their evolutions are analyzed using common neighbor analysis (CNA) (Honeycutt and Andersen, 1987; Stukowski, 2012) and are visualized using OVITO software (Stukowski, 2010) which provides detailed microstructural evolution during the phase transition. The blue, red, and gray atoms represent the austenite atoms in B2 structure, the martensite atoms in B19′structure, and the disordered atoms in metastable state. All simulations are performed by the open source LAMMPS code (Plimpton, 1995).

3. Calculations of energy and stress

Based on 2NN MEAM potential, the total energy of a system is approximated as (Ko et al., 2015)

$$E_{total} = \sum_i \left[F_i(\overline{\rho}_i) + \frac{1}{2} \sum_{j(\neq i)} s_{ij}\varphi_{ij}(r_{ij}) \right] \quad (1)$$

where F_i is the embedding energy as a function of background electron density$\overline{\rho}_i$, $s_{ij}$and $\phi_{ij}(r_{ij})$ are the screening function and the pair interaction between atoms i and j separated by a distance r_{ij} .

Table 1
The information of NC NiTi models with different grain sizes.

Grain size/nm	4.02	7.98	11.97
Number of grains	64	27	27
Number of atoms	157305	521554	1763366
Models	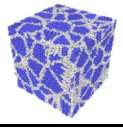	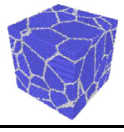	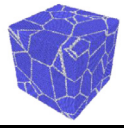

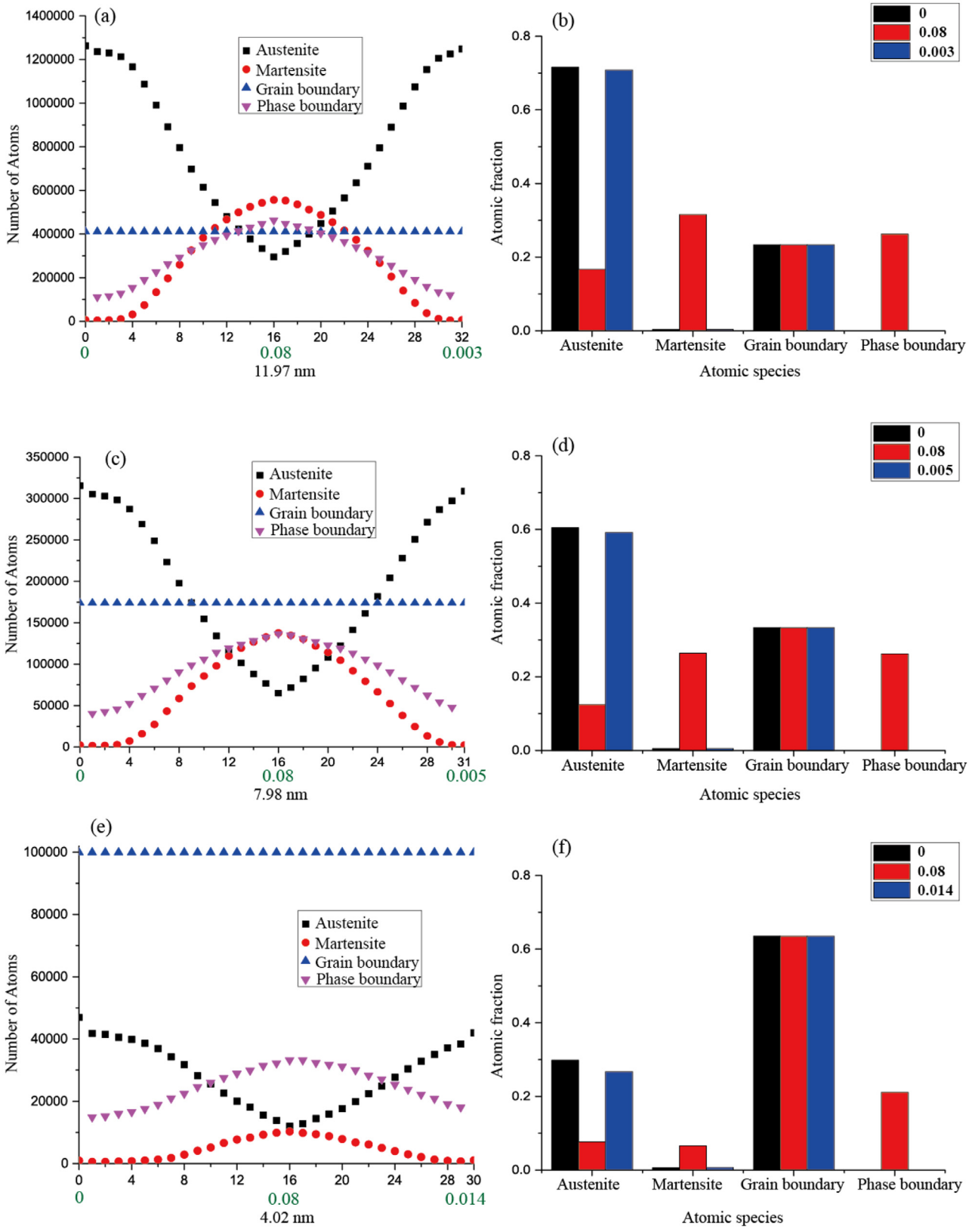

Fig. 3. The variation of the number of atoms during loading and unloading in the samples with grain size of (a) 11.97; (c) 7.98; (e) 4.02 nm; The atomic fraction of Austenite (B2), Martensite (B19′), grain boundary and phase boundary in the sample with grain size of (b) 11.97 nm (ε=0 → ε=0.08 → ε=0.003); (d) 7.98 nm (ε=0 → ε=0.08 → ε=0.005); and (f) 4.02 nm (ε=0 → ε=0.08 → ε=0.014).

Please cite this article as: K. Nie, M.-P. Li and W.-P. Wu et al., Grain size-dependent energy partition in phase transition of NiTi shape memory alloys studied by molecular dynamics simulation, International Journal of Solids and Structures, https://doi.org/10.1016/j.ijsolstr.2020.02.027

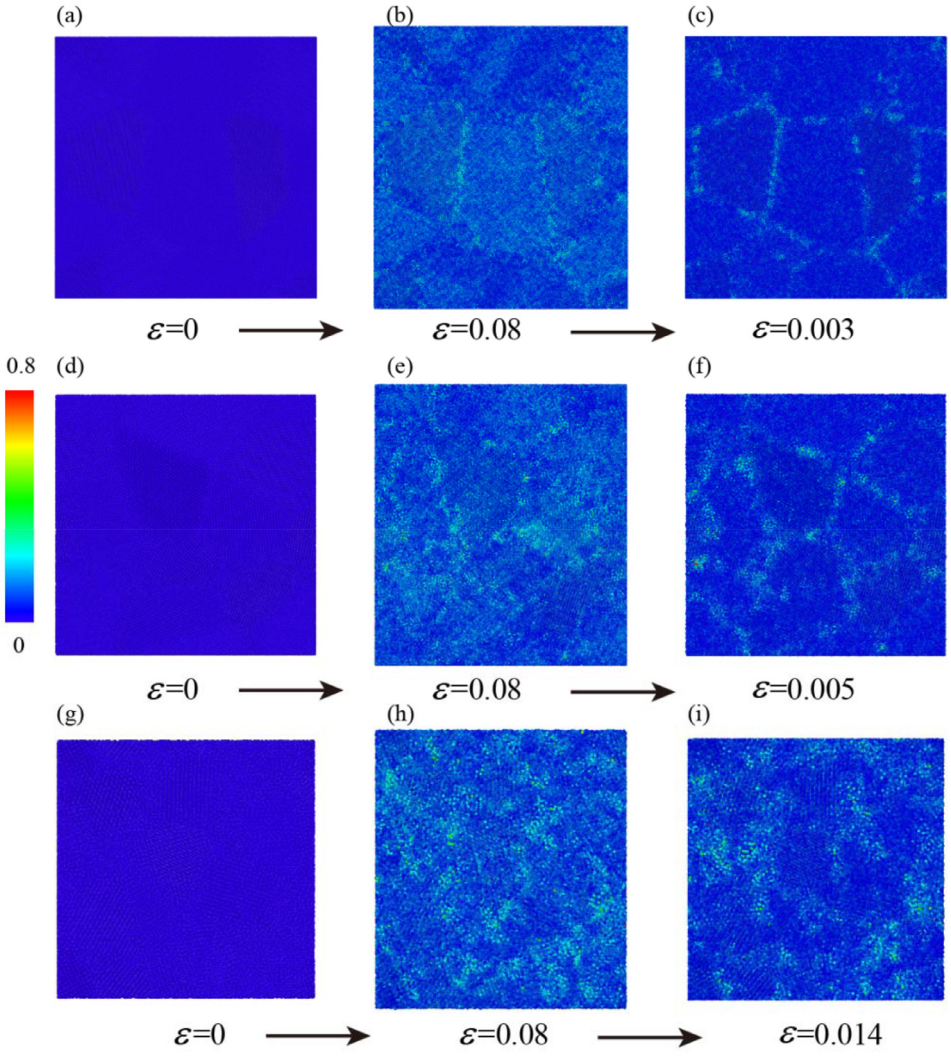

Fig. 4. The distribution of local shear strain in the samples with grain size of 11.97 nm ((a)–(c)), 7.98 nm ((d)–(f)), 4.02 nm ((g)–(i)).

In MD simulation, the kinetic energy at a given thermodynamic temperature can be expressed as

$$E_k = \frac{3NK_B}{2}T \tag{2}$$

where K_B is Boltzmann constant, N is the number of atoms. The kinetic energy is stable at constant temperature, the change of potential energy is consistent with the change of total energy.

The forces on each atom can be determined by the energy in MD simulation. At each atom the dipole force tensor β_{ij} is given by (Horstemeyer, 2012)

$$\beta_{km}^{i} = \frac{1}{\Omega^i}\sum_{j\neq(i)}^{N} f_k^i\left(r^{ij}\right)r_m^{ij} \tag{3}$$

where i refers to the atom in question and j refers to the neighboring atom, f_k is the force vector between atoms, r_m is a displacement vector between atoms i and j, N is the number of nearest neighbor atoms, and Ω^i is the undeformed atomic volume. Since stress is defined at a continuum point, we determine the stress tensor as a volume average over the block of material,

$$\sigma_{mk} = \frac{1}{N^*}\sum_{i}^{N^*}\beta_{mk}^{i} \tag{4}$$

in which the stress tensor is defined in terms of the total number of atoms N^* in the block of material. We use this averaged stress to determine the stress–strain response and yielding of the block of material.

Since the kinetic energy is stable for the simulation conducted at constant temperature, the potential energy (the total energy minus the kinetic energy) of each atom is quantified and is used to describe the phase transition behavior. To reveal the underlying physical mechanism, all the atoms are classified into the four types: austenite, martensite, grain boundary, and phase boundary. The phase boundary atoms and grain boundary atoms are distinguished in post processing. During loading and unloading, the disordered atoms which appear in the crystallite are identified as phase boundary atoms.

4. Results and discussion

4.1. Grain size effects on σ-ε behavior, microstructure and deformation mechanisms

The microstructure images during phase transition are presented in Fig. 1. The austenite atoms transform into martensite atoms in loading, then the reverse process occurs in unloading in samples with grain size of 11.97 and 7.98 nm. However, it is observed in sample with grain size of 4.02 nm that part of

Please cite this article as: K. Nie, M.-P. Li and W.-P. Wu et al., Grain size-dependent energy partition in phase transition of NiTi shape memory alloys studied by molecular dynamics simulation, International Journal of Solids and Structures, https://doi.org/10.1016/j.ijsolstr.2020.02.027

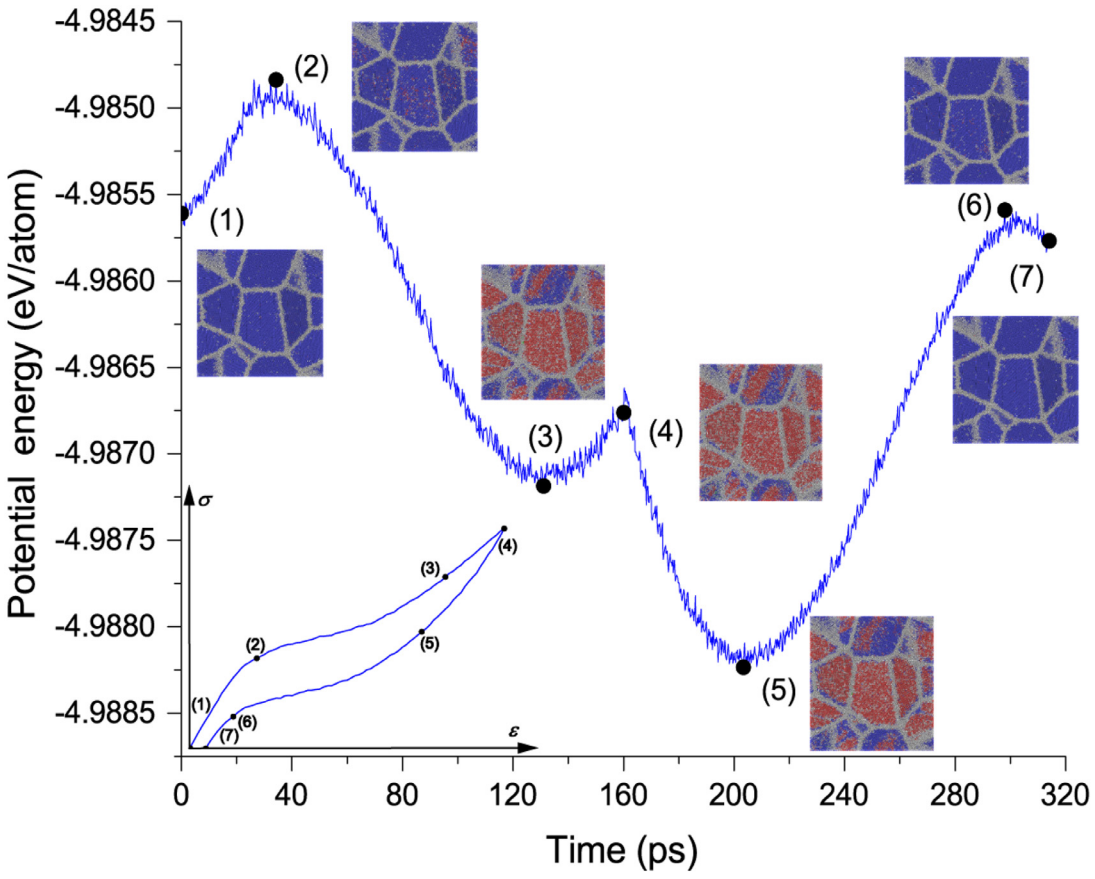

Fig. 5. The time (or strain) vs. average potential energy curve, the stress–strain curve and the microstructure snapshots for sample with grain size of 11.97 nm. The loading process is from point 1 to point 4, and the unloading process is from point 4 to point 7.

austenite atoms nearby grain boundary and in the grain inside transform into metastable atoms (gray atoms) during loading, then the reverse phase transition occurs during unloading. This indicates that the parent phase of those metastable atoms are austenite atoms and partial austenite atoms experience incomplete phase transition (Ahadi and Sun, 2015; Ko et al., 2017). This phenomenon has not been observed in the phase transition behavior in sample with grain size of 11.97 nm. The incomplete phase transition appears, and complete phase transition phenomenon disappears in samples with decreasing grain size.

As shown in the stress–strain curves of Fig. 2, the maximum stress increasing with decrease in grain size. The phase transition strain decreases under the same stress level with decrease in grain size. It means that the strength and the phase transition stress are increased with decreasing grain size and it is more difficult to induce phase transition by stress with decrease in grain size. The phenomenon is consistent with the experimental results (Sun et al., 2014; Waitz et al., 2004).

During loading, the number of martensite atoms increases, and number of austenite atoms decreases when phase transition (austenite → martensite) is induced as shown in Fig. 3. It is found that, with decreasing grain size, the fraction of martensite atoms decreases from the same strain of 8%. The formed martensite atoms only account for 6.6% in the sample with grain size of 4.02 nm andε = 0.08. It means that when grain size is reduced, the atoms experiencing phase transition process become less and less.

The number of grain boundary atoms remains constant in all the samples during loading and unloading. The grain boundary atoms do not experience phase transition process, so the role of grain boundary is different with the atoms in B2 and $B19'$ structures. The fraction of grain boundary atoms increases from 23.33% to 33.33%, and then to 63.51% with decreasing grain size. The grain boundary becomes an important part of the NC system with smaller grain size. The effects of such grain boundary dominance on the phase transition behavior will be discussed in the following sections.

The atomic level shear strain is a good measure of deformation (Shimizu et al., 2007), which can help to understand the mechanical properties and phase transition behavior in NC NiTi. From Fig. 4(b) (e) (h), it is seen that the shear strain exists in both the crystallite and grain boundary at ε=0.08 and the main lattice deformation is shear during martensitic phase transition. Owing to the reversible phase transition process (austenite↔martensite), the shear strain in crystallite atoms recover after the unloading of the samples (grain size = 11.97, 7.98 nm see from Fig. 4(c) and (f)). However, there is no obvious shear deformation inside the grains of the sample with grain size of 4.02 nm atε=0.08. After unloading, it is found that the plastic shear strain is almost concentrated on the grain boundary in each sample (see Fig. 4), which indicated that grain boundary sliding is the main plastic deformation mechanism and that the plastic shear strain increases with the decrease of the grain size (see Fig. 2). Therefore, the phase transition is suppressed gradually with decrease in grain size.

4.2. Grain size effects on potential energy and microstructure evolution

In this section, the potential energy per atom is calculated and is used to interpret the calculated phase transition responses. The time of loading-and-unloading (or strain) vs. potential energy

Please cite this article as: K. Nie, M.-P. Li and W.-P. Wu et al., Grain size-dependent energy partition in phase transition of NiTi shape memory alloys studied by molecular dynamics simulation, International Journal of Solids and Structures, https://doi.org/10.1016/j.ijsolstr.2020.02.027

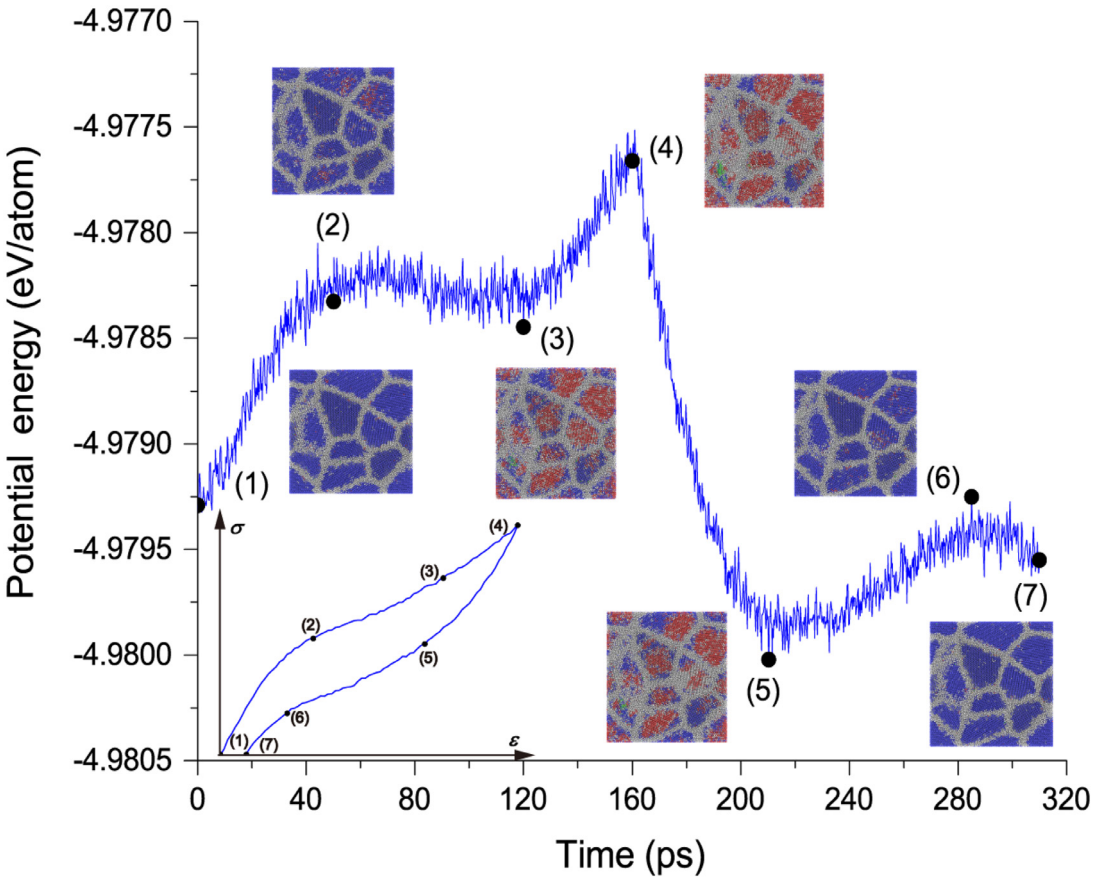

Fig. 6. The time (or strain) vs. average potential energy curve, the stress–strain curve and the microstructure snapshots for sample with grain size of 7.98 nm. The loading process is from point 1 to point 4, and the unloading process is from point 4 to point 7.

curve, stress–strain curve and the corresponding microstructure images are shown in Figs. 5–7, respectively.

As usual, the potential energy increases during loading due to the positive work done by external force, and deceases during unloading. However, it is worth noting that the phase transition behavior leads to the emergence of opposite phenomenon. The potential energy decreases in loading or increases in unloading due to phase transition. Austenite atoms transform into martensite atoms in the martensitic phase transition process. And the potential energy of austenite atoms is higher than that of martensite atoms. It is found that the potential energy evolution varies significantly with decreasing grain size from Figs. 5–7.

4.2.1. Results of samples with grain size of 11.97 nm and 7.98 nm

As shown in Fig. 5, the loading process consists of three stages. **Stage I (point 1 to point 2).** Owing to the work done by the external force, potential energy increases monotonically at elastic tensile deformation stage. Then the slope of stress–strain curve begins to decrease rapidly due to the martensitic phase transition and a few martensite can be observed inside the grains in the microstructure snapshot. The fraction of martensite atoms is only 1.8%. **Stage II (point 2 to point 3).** As shown in Fig. 5, the potential energy begins to decrease because martensitic phase transition proceeds over a wide range in this stage. Many austenite atoms are transformed into martensite atoms, so the potential energy decreases. It is seen that many martensite atoms appear inside the grains in the microstructure snapshot, the fraction of martensite is 28.36%. **Stage III (point 3 to point 4).** In this stage, the potential energy increases again because phase transition process is getting saturated and the martensite morphology shows a little change.

The unloading process consists of stages IV, V, and VI (point 4 to point 5, point 5 to point 6, and point 6 to point 7), respectively. Due to the negative work done by external force in stage IV and VI, potential energy decreases in these two stages of unloading. The reverse phase transition (-martensite → austenite) in stage V leads to the increase of the potential energy. It is seen from Fig. 5 that many martensite atoms transform back into austenite atoms in the microstructure snapshots in point 5 and 6, the fraction of martensite atoms decreases from 27.69% to 0.7%. The slope in stress–strain curve also decreases because the phase transition takes place over a wide range in this stage of unloading.

For the sample with grain size of 7.98 nm, the evolution of time vs. potential energy curve, stress–strain curve, and microstructure snapshots in stages I, III, IV, V, and VI in Fig. 6 show a similar trend with those of the sample (11.97 nm) in Fig. 5 but only with quantitative differences. For example, the martensite appears in the middle of the grains and then spreads to the grain boundary. Also, due to the suppression of phase transition for the smaller grain size sample, some austenite atoms are still observed at ε=0.08 as shown in the microstructure snapshot of Fig. 6.

4.2.2. Results of the sample with grain size of 4.02 nm

Potential energy evolution shows drastic change for the sample with grain size of 4.02 nm as shown in Fig. 7. The potential energy increases/decreases monotonically during loading/unloading. Compared with the case of grain size of 11.97 and 7.98 nm, there is no drastic change in the slope of stress–strain curve. From the microstructure snapshots in point 1–3, it is seen that only few martensite atoms appear at the end of loading, which indicates that the volume and energy of grain boundary become dominant

Please cite this article as: K. Nie, M.-P. Li and W.-P. Wu et al., Grain size-dependent energy partition in phase transition of NiTi shape memory alloys studied by molecular dynamics simulation, International Journal of Solids and Structures, https://doi.org/10.1016/j.ijsolstr.2020.02.027

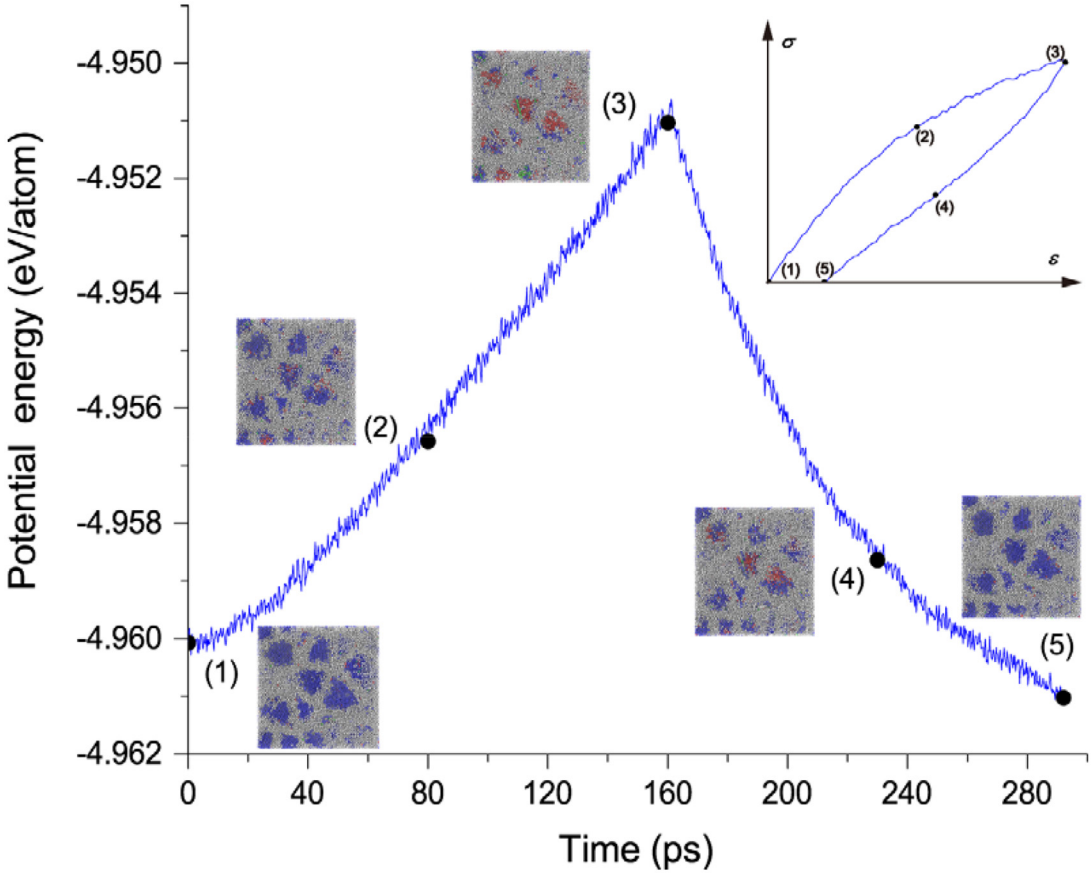

Fig. 7. The time (or strain) vs. average potential energy curve, the stress–strain curve and the microstructure snapshots for sample with grain size of 4.02 nm. The loading process is from point 1 to point 3, and the unloading process is from point 3 to point 5.

Table 2
Variation of potential energy per atom for each component (austenite, martensite, grain boundary and phase boundary) in loading.

Variation of potential energy (eV)	Austenite	Martensite	Grain boundary	Phase boundary
11.97 nm	-3.38×10^{-3}	-1.25×10^{-2}	1.21×10^{-2}	2.55×10^{-3}
7.98 nm	-3.14×10^{-3}	-1.19×10^{-2}	1.19×10^{-2}	4.76×10^{-3}
4.02 nm	1.44×10^{-3}	-5.47×10^{-3}	1.07×10^{-2}	1.19×10^{-2}

and the suppressed phase transition leads to monotonic variation of potential energy. The fraction of martensite atoms is only 6.6% for the sample with grain size of 4.02 nm. Compared with Section 4.2.1, it is seen that phase transition is almost totally suppressed for sample with grain size of 4.02 nm. The trend of the potential energy evolution shows a significant grain size dependence, from the non-monotonic variation for the samples with grain size of 11.97 and 7.98 nm to the monotonic variation for the sample with grain size of 4.02 nm. The details of the energy partition are given below.

4.3. Grain size effects on energy partition

The variations of each energy term per atom during loading are listed in Table 2. To show the role of each component (austenite, martensite, grain boundary, and phase boundary) during phase transition process, the pie chart of the energy partition among different energy terms is shown in Fig. 8.

For the austenite atoms, owing to their small atomic fraction at ε=0.08 at the end of the loading (shown in Fig. 3), their contribution to the variation of total potential energy is small, and the percentage is less than 10% in all the samples.

For the phase boundary atoms, the number of atoms increases/decreases in loading/unloading monotonically. At^ε=0.08, the phase boundary atoms separate martensite atoms in the samples with grain size of 11.97, and 7.98 nm as shown in Fig. 1. Owing to the lattice distortion, the contribution of phase boundary to the total potential energy is 8.37% for sample with grain size of 11.97 nm and 14.27% for sample with grain size of 7.98 nm. For sample with grain size of 4.02 nm, the phase boundary atoms are located near the grain boundary and in the interior of the grain. The fraction of phase boundary atoms is about 20%. So the contribution of phase boundary atoms to the total variation of potential energy increases with the decrease of grain size from 8.37% to 14.27% then to 25.77%.

For the grain boundary atoms, their potential energy increases/decreases monotonically during loading/unloading. The potential energy increase of each grain boundary atom is about 1.0×10^{-2}eV due to the external work input, showing no obvious difference for all the three samples. However, the fraction of grain boundary atoms increases with decreasing grain size, Therefore, the contribution of grain boundary atoms to the variation of total system potential energy increases with the decrease of grain size. The percent increases from 35.19% for sample with grain

Please cite this article as: K. Nie, M.-P. Li and W.-P. Wu et al., Grain size-dependent energy partition in phase transition of NiTi shape memory alloys studied by molecular dynamics simulation, International Journal of Solids and Structures, https://doi.org/10.1016/j.ijsolstr.2020.02.027

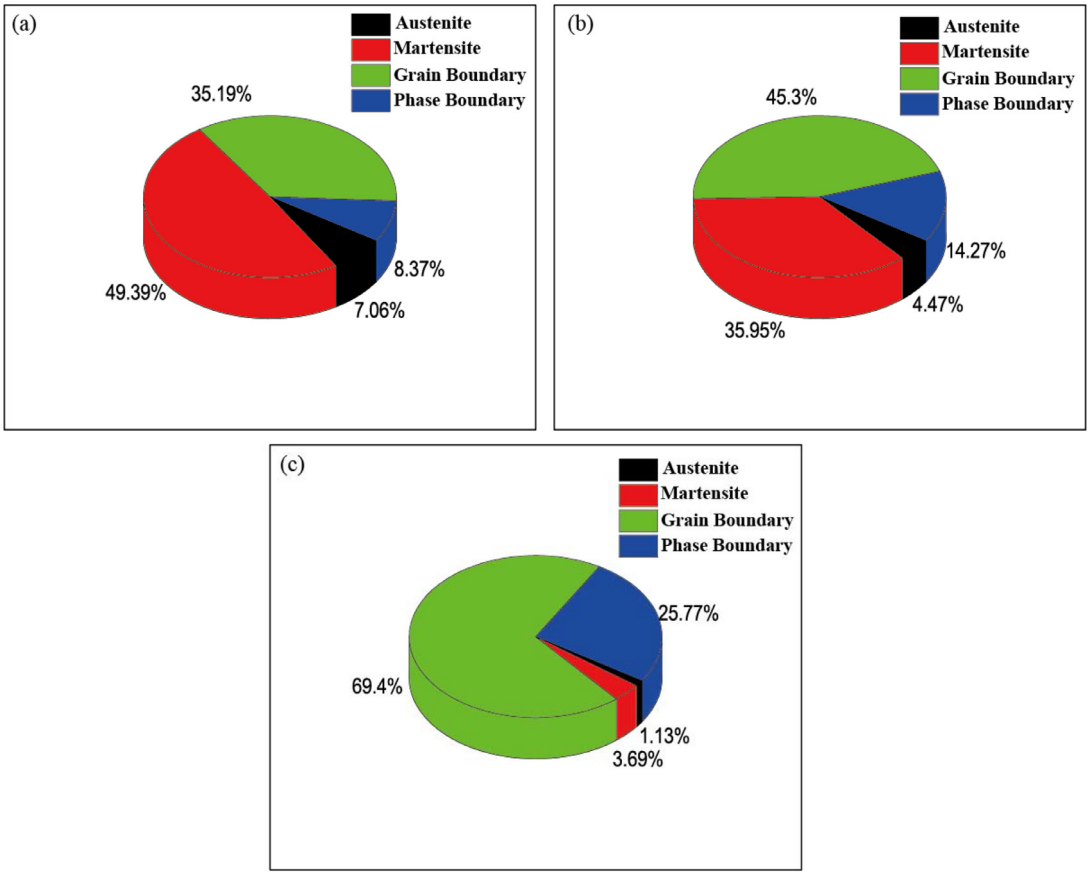

Fig. 8. Energy partition in each component (Austenite, Martensite, grain boundary and phase boundary) in the samples with grain size of (a) 11.97, (b) 7.98, and (c) 4.02 nm.

size of 11.97 nm to 45.3% for sample with grain size of 7.98 nm, then to 69.4% for sample with grain size of 4.02 nm. The results are in agreement with the continuum-based theoretical predictions (Li and Sun, 2018).

For the martensite atoms, as their number increases, the total potential energy decreases due to phase transition (austenite → martensite) during loading and vice versa. With decrease in grain size shown in Table 2, it is found that the decrement of potential energy of martensite atom decreases. Obviously, the martensite atoms with more decrement in energy are more stable. It means that it is more difficult to generate the stable martensite atoms in the smaller grain size sample. On the other hand, it can be found that the decrement of potential energy for austenite atoms also decreases and even becomes positive with decreasing grain size. It means the atoms in B2 structure become more stable in the sample with smaller grain size. Therefore, it can be inferred that the phase transition is suppressed gradually when grain size is reduced. Meanwhile, it is found that the increment of potential energy for grain boundary and phase boundary atoms is positive, and that for martensite atoms is negative in loading. With the decrease of grain size, the contribution of martensite atoms decreases from 49.39% to 35.95%, and then to 3.69%, meanwhile that of grain boundary increases from 35.19% to 45.3%, and then to 69.4% (see Fig. 8).

To summarize, when the grain size is large, the martensite atoms dominate the total potential energy evolution and play a dominant role in the phase transition behavior of NC NiTi. The total potential energy decreases as the phase transition proceeds during loading for the samples with grain size of 11.97, and 7.98 nm. When the grain size is reduced down to a few nanometers, the volume fraction of grain boundary atoms increases significantly, which results in the monotonic increase of the system potential energy for the sample with grain size of 4.02 nm. The increase of grain boundary energy dominates the variation of the system potential energy among all the energy terms (austenite, martensite, grain boundary and phase boundary). It is seen that the grain boundary plays an increasingly important role in phase transition energetics and behavior of NC NiTi as the grain size is reduced. The grain boundary energy dominates the total potential energy variation and leads to the monotonical variation of the potential energy in the nano-sized grain.

4.4. Grain size effects on energy dissipation

From the stress–strain curves in Figs. 5(a) 6(a) 7(a), the system dissipates mechanical energy in the loading-and-unloading cycle. With decreasing grain size, the dissipated energy per atom increases as shown in Table 3. Fig. 9 shows the proportion of dissipated energy in each component. It is seen that both crystallite atoms (including austenite, martensite) and grain boundary atoms dissipate energy. There are two energy dissipation mechanisms: the atomic interface friction in phase transition process and plastic dissipation caused by grain boundary sliding.

Table 3
The dissipated energy per atom after unloading in the samples of different grain sizes.

Grain size/nm	11.97	7.98	4.02
Dissipated potential energy per atom/eV	1.80×10^{-4}	2.60×10^{-4}	9.80×10^{-4}

Please cite this article as: K. Nie, M.-P. Li and W.-P. Wu et al., Grain size-dependent energy partition in phase transition of NiTi shape memory alloys studied by molecular dynamics simulation, International Journal of Solids and Structures, https://doi.org/10.1016/j.ijsolstr.2020.02.027

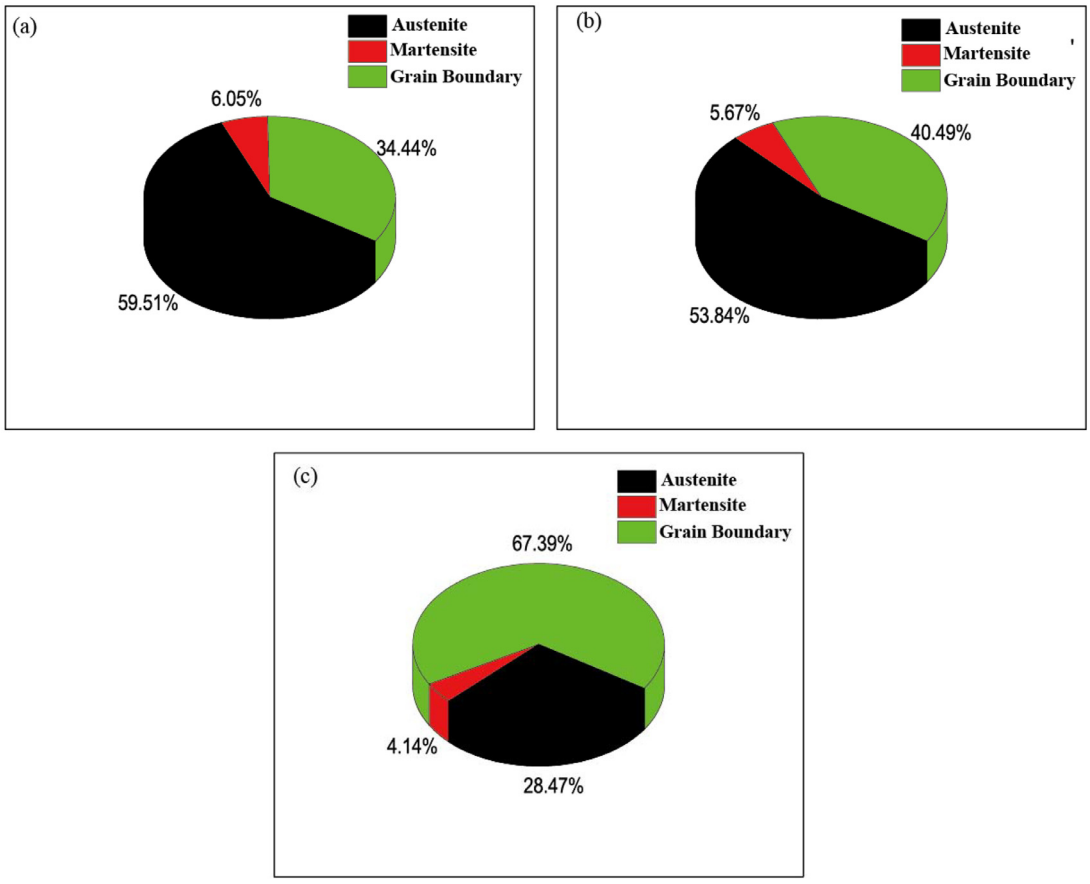

Fig. 9. Dissipated energy in each component (Austenite, Martensite, and grain boundary) in the samples with grain size of (a) 11.97, (b) 7.98, and (c) 4.02 nm.

When the grain size is reduced, the suppression of phase transition causes a significant increase of the applied stress at ε=0.08 (see Fig. 2). This activates significant grain boundary motions. The dissipated energy from grain boundary sliding becomes dominant and accounts for 67.39% of the total dissipation in the sample with grain size of 4.02 nm as shown in Fig. 9, While the energy dissipated from phase transition process becomes minor. The results of Fig. 9 show that, for givenε=0.08, with decreasing grain size, the proportion of dissipated energy of austenite atoms decreases from 59.51% to 28.47%. It is expected that the main energy dissipation mechanism changes from the atomic interface friction of phase transition process to plastic deformation caused by grain boundary sliding with decrease of grain size.

5. Summary and conclusions

In this paper, detailed evolutions of microstructure and energetics (potential energy, energy partition, and energy dissipation) of NC NiTi during stress-induced phase transition process at atomic level are obtained by the MD simulations. The investigation revealed the underlying mechanism of the experimentally observed strong grain size effects on phase transition behavior of NC NiTi. The following conclusions can be drawn from the present study:

1. The phase transition under stress in NC NiTi is gradually suppressed and the fraction of the transformed martensite atoms decreases with decrease of the grain size. Phase transformation stress increases significantly with the decrease in grain size. Partial phase transition inside nano-sized crystallites is observed due to the stabilization effect of the grain boundary constraint in the NiTi sample with grain size of 4.02 nm.
2. The microstructure evolution and the potential energy landscape change a lot with the decrease of grain size, which significantly affects stress–strain response. The strain softening behavior typically observed in phase transition of coarse-grained samples disappears in the sample with nano-scale grain size. When the grain size is reduced down to several nanometers, the potential energy curve of the system become convex and varies monotonically with applied strain in loading and unloading.
3. The contribution of the NiTi crystallite phases (austenite and martensite) to the total potential energy and its variation decreases with decreasing grain size, while the contribution of the interfacial phases (especially grain boundary) become dominant when the grain size is reduced down to several nanometers in the nanocrystal system. Such interfacial dominance brings a “nonconvex-to-convex” change of the system energy, which significantly affect the material behavior and the energy dissipation during phase transition. In addition, with decreasing grain size, the energy dissipation mechanism at nano-scale also involve plastic deformation by grain boundary sliding.

Declaration of Competing Interest

The authors declare that there is no conflict of interest regarding the publication of this paper.

Acknowledgements

The work was supported by the National Natural Science Foundation of China (through grant Nos. 11532010 and 11772236), and the RGC of Hong Kong SAR (through GRF grant No. 16215218).

Please cite this article as: K. Nie, M.-P. Li and W.-P. Wu et al., Grain size-dependent energy partition in phase transition of NiTi shape memory alloys studied by molecular dynamics simulation, International Journal of Solids and Structures, https://doi.org/10.1016/j.ijsolstr.2020.02.027

K. Nie would like to thank Dr. Xian-Long Zhang for useful discussion about paper writing.

References

Ahadi, A., Matsushita, Y., Sawaguchi, T., Sun, Q.P., Tsuchiya, K., 2017. Origin of zero and negative thermal expansion in severely-deformed superelastic NiTi alloy. Acta Mater. 124, 79–92.
Ahadi, A., Sun, Q.P., 2013. Stress hysteresis and temperature dependence of phase transition stress in nanostructured NiTi—effects of grain size. Appl. Phys. Lett. 103, 021902.
Ahadi, A., Sun, Q.P., 2014. Effects of grain size on the rate-dependent thermomechanical responses of nanostructured superelastic NiTi. Acta Mater. 76, 186–197.
Ahadi, A., Sun, Q.P., 2015. Stress-induced nanoscale phase transition in superelastic NiTi by in situ X-ray diffraction. Acta Mater. 90, 272–281.
Ahadi, A., Sun, Q.P., 2016. Grain size dependence of fracture toughness and crack-growth resistance of superelastic NiTi. Scripta Mater. 113, 171–175.
Chen, X., Lu, S., Zhao, Y., Fu, T., Huang, C., Peng, X.H., 2017. Molecular dynamic simulation on nano-indentation of NiTi SMA. Mater. Sci. Eng. A 712, 592–602.
Chowdhury, P., Ren, G., Sehitoglu, H., 2015. NiTi superelasticity via atomistic simulations. Phil. Mag. Lett. 95, 574–586.
Dong, L., Sun, Q.P., 2009. Stress hysteresis and domain evolution in thermoelastic tension strips. Acta Mech. Solida Sin. 22, 399–406.
Dong, L., Zhou, R.H., Wang, X.L., Hu, G.K., Sun, Q.P., 2016. On interfacial energy of macroscopic domains in polycrystalline NiTi shape memory alloys. Int. J. Solids Struct. 80, 445–455.
Duerig, T., Pelton, A., Stöckel, D., 1999. An overview of nitinol medical applications. Mater. Sci. Eng. A 273-275, 149–160.
Honeycutt, J.D., Andersen, H.C., 1987. Molecular dynamics study of melting and freezing of small Lennard-Jones clusters. J. Phys. Chem. 91, 4950–4963.
Horstemeyer, M.F., 2012. Integrated Computational Materials Engineering (ICME) for Metals: Using multiscale Modeling to Invigorate Engineering Design With Science. Wiley-TMS, New York, United States, pp. P146–P163.
Humbeeck, J.V., 1999. Non-medical applications of shape memory alloys. Mater. Sci. Eng. A 273-275, 134–148.
Ko, W.S., Grabowski, B., Neugebauer, J., 2015. Development and application of a Ni-Ti interatomic potential with high predictive accuracy of the martensitic phase transition. Phys. Rev. B 92, 134107.
Ko, W.S., Maisel, S.B., Grabowski, B., Jeon, J.B., Neugebauer, J., 2017. Atomic scale processes of phase transformations in nanocrystalline NiTi shape-memory alloys. Acta Mater. 123, 90–101.
Li, M.P., Sun, Q.P., 2018. Nanoscale phase transition behavior of shape memory alloys—closed form solution of 1D effective modelling. J. Mech. Phys. Solids 110, 21–37.
Ma, G.F., Qin, S.J., Shang, J.X., Wang, F.H., Chen, Y., 2017. Atomistic study on the phase transformation in NiTi under thermal cycling. J. Alloys Compd. 705, 218–225.
Mao, S.C., Luo, J.F., Zhang, Z., Wu, M.H., Liu, Y., Han, X.D., 2010. EBSD studies of the stress-induced B2–B19′ martensitic transformation in NiTi tubes under uniaxial tension and compression. Acta Mater. 58, 3357–3366.
Miyazaki, S., Imai, T., Otsuka, K., Suzuki, Y., 1981. Lüders-like deformation observed in the transformation pseudoelasticity of a Ti-Ni alloy. Scripta Metall. 15, 853–856.
Morgan, N.B., 2004. Medical shape memory alloy applications—the market and its products. Mater. Sci. Eng. A 378, 16–23.
Mousavi, T., Karimzadeh, F., Abbasi, M.H., 2008. Synthesis and characterization of nanocrystalline NiTi intermetallic by mechanical alloying. Mater. Sci. Eng. A 487, 46–51.
Muralles, M., Park, S.D., Kim, S.Y., Lee, B., 2017. Phase transformations, detwinning and superelasticity of shape-memory NiTi from MEAM with practical capability. Comput. Mater. Sci. 130, 138–143.
Plimpton, S., 1995. Fast parallel algorithms for short-range molecular dynamics. J. Comput. Phys. 117, 1–19.
Reedlunn, B., Churchill, C.B., Nelson, E.E., Shaw, J.A., Daly, S.H., 2014. Tension, compression, and bending of superelastic shape memory alloy tubes. J. Mech. Phys. Solids 63, 506–537.
Saadat, S., Salichs, J., Noori, M., Hou, Z., Davoodi, H., Bar-on, I., Suzuki, Y., masuda, A., 2002. An overview of vibration and seismic applications of NiTi shape memory alloy. Smart Mater. Struct. 11, 218–229.
Shaw, J.A., Kyriakides, S., 1997. On the nucleation and propagation of phase transformation fronts in a NiTi alloy. Acta Mater. 45, 683–700.
Shimizu, F., Ogata, S., Li, J., 2007. Theory of shear banding in metallic glasses and molecular dynamics calculations. Mater. Trans. 48, 2923–2927.
Stukowski, A., 2010. Visualization and analysis of atomistic simulation data with OVITO-the Open Visualization Tool. Model. Simul. Mater. Sci. Eng. 18, 015012.
Stukowski, A., 2012. Structure identification methods for atomistic simulations of crystalline materials. Model. Simul. Mater. Sci. Eng. 20, 045021.
Sun, Q.P., Ahadi, A., Li, M.P., Chen, M.X., 2014. Effects of grain size on phase transition behavior of nanocrystalline shape memory alloys. Sci. China Technol. Sci. 57, 671–679.
Truskinovsky, L., Zanzotto, G., 1996. Ericksen's bar revisited: energy wiggles. J. Mech. Phys. Solids 44, 1371–1408.
Ueland, S.M., Schuh, C.A., 2013. Grain boundary and triple junction constraints during martensitic transformation in shape memory alloys. J. Appl. Phys. 114, 053503.
Waitz, T., Kazykhanov, V., Karnthaler, H.P., 2004. Martensitic phase transformations in nanocrystalline NiTi studied by TEM. Acta Mater. 52, 137–147.
Waitz, T., Tsuchiya, K., Antretter, T., Fischer, F.D., 2009. Phase transformations of nanocrystalline martensitic materials. MRS Bull. 34, 814–821.
Wang, B., Kang, G.Z., Kan, Q.H., Zhou, K., Yu, C., 2017. Molecular dynamics simulations to the pseudo-elasticity of NiTi shape memory alloy nano-pillar subjected to cyclic compression. Comput. Mater. Sci. 191, 132–138.
Yin, Q.Y., Wu, X.Q., Huang, C.G., Wang, X., Wei, Y.P., 2015. Atomistic study of temperature and strain rate-dependent phase transformation behaviour of NiTi shape memory alloy under uniaxial compression. Philos. Mag. 95, 2491–2512.
Yin, H., He, Y.J., Moumni, Z., Sun, Q.P., 2016. Effects of grain size on tensile fatigue life of nanostructured NiTi shape memory alloy. Int. J. Fatigue 88, 166–177.
Zhong, Y., Gall, K., Zhu, T., 2012. Atomistic characterization of pseudoelasticity and shape memory in NiTi nanopillars. Acta Mater. 60, 6301–6311.

Please cite this article as: K. Nie, M.-P. Li and W.-P. Wu et al., Grain size-dependent energy partition in phase transition of NiTi shape memory alloys studied by molecular dynamics simulation, International Journal of Solids and Structures, https://doi.org/10.1016/j.ijsolstr.2020.02.027